HHS Public Access

Author manuscript

Kidney Int. Author manuscript; available in PMC 2015 February 01.

Published in final edited form as:

Kidney Int. 2014 August ; 86(2): 327–337. doi:10.1038/ki.2014.64.

The chemokine receptor CXCR6 contributes to recruitment of bone marrow-derived fibroblast precursors in renal fibrosis

Yunfeng Xia[1,2], **Jingyin Yan**[1], **Xiaogao Jin**[1], **Mark L. Entman**[3], and **Yanlin Wang**[1,4,*]

[1]Division of Nephrology, Department of Medicine, Baylor College of Medicine, Houston Texas, USA

[2]Division of Nephrology, Department of Medicine, Guangdong General Hospital and Guangdong Academy of Medical Sciences, Guangzhou, China

[3]Division of Cardiovascular Sciences and the DeBakey Heart Center, Department of Medicine, Baylor College of Medicine and The Methodist Hospital, Houston, Texas, USA

[4]Medical Care Line, Michael E. DeBakey Veterans Affairs Medical Center, Houston, Texas, USA

Abstract

Bone marrow-derived fibroblasts in circulation are of hematopoietic origin, proliferate, differentiate into myofibroblasts, and express the chemokine receptor CXCR6. Since chemokines mediate the trafficking of circulating cells to sites of injury, we studied the role of CXCR6 in mouse models of renal injury. Significantly fewer bone marrow-derived fibroblasts accumulated in the kidney of CXCR6 knockout mice in response to injury, expressed less profibrotic chemokines and cytokines, displayed fewer myofibroblasts, and expressed less α-smooth muscle actin in the obstructed kidneys compared with wild-type mice. CXCR6 deficiency inhibited total collagen deposition and suppressed expression of collagen I and fibronectin in the obstructed kidneys. Furthermore, wild type mice engrafted with $CXCR6^{-/-}$ bone marrow cells displayed fewer bone marrow-derived fibroblasts in the kidneys with obstructive injury and showed less severe renal fibrosis compared with wild-type mice engrafted with $CXCR6^{+/+}$ bone marrow cells. Transplant of wild type bone marrow into $CXCR6^{-/-}$ recipients restored recruitment of myeloid fibroblasts and susceptibility to fibrosis. Hematopoietic fibroblasts migrate into injured kidney and proliferate and differentiate into myofibroblasts. Thus, CXCR6, together with other chemokines and their receptors, may play important roles in the recruitment of bone marrow-derived fibroblast precursors into the kidney and contribute to the pathogenesis of renal fibrosis.

[*]**Corresponding author:** Yanlin Wang, MD, PhD, Department of Medicine-Nephrology, Baylor College of Medicine, One Baylor Plaza, BCM395, Houston TX 77030, Tel: 713-798 3689, FAX: 713-798 5010, yanlinw@bcm.edu.

DISCLOSURES

None

INTRODUCTION

Chronic kidney disease is a global public health problem[1]. Renal fibrosis is the final common manifestation of chronic kidney disease leading to end stage renal disease[2, 3]. Renal interstitial fibrosis is characterized by fibroblast activation and excessive production and deposition of extracellular matrix (ECM), which results in destruction of renal parenchyma and causes progressive loss of kidney function. Because activated fibroblasts are responsible for ECM production, their activation is regarded as a key event in the pathogenesis of renal fibrosis[4–6]. However, the origin of these fibroblasts has been controversial. They are traditionally thought to arise from resident renal fibroblasts. Accumulating evidence indicates that they may originate from bone marrow-derived fibroblast progenitor cells[7–12].

Circulating fibroblast precursors termed fibrocytes are derived from a subpopulation of monocytes via monocyte-to-fibroblast transition[12–16]. These cells express mesenchymal markers such as collagen I and vimentin and hematopoietic markers such as CD45 and CD11b[13, 16–19]. These cells in culture display an adherent, spindle-shape morphology and express α smooth muscle actin (α-SMA) that is enhanced when cells are treated with TGF-β1, consistent with the concept that they can differentiate into myofibroblasts[17–19]. The differentiation of these cells is regulated by cytokines. Profibrotic cytokines - IL-4 and IL-13 promote myeloid fibroblast differentiation, whereas antifibrotic cytokines - IFN-γ and IL-12 inhibit its differentiation[15, 20]. However, the molecular mechanisms underlying recruitment of these cells into injured kidneys are incompletely understood.

Chemokines play primary roles in mediating the trafficking of circulating cells to sites of injury via activation of their seven-transmembrane G protein-coupled receptors[21]. We have recently shown that circulating fibroblast precursors express the chemokine receptor CXCR6[11]. In the present study, we investigated the role of CXCR6 in renal fibrosis using CXCR6 knockout (KO) mice. Our results showed that CXCR6 deficiency inhibited the development of renal fibrosis through suppression of myeloid fibroblast precursor infiltration into the kidney.

RESULTS

Characterization of Bone Marrow-derived Fibroblasts

We have shown that bone marrow-derived fibroblast precursors migrated into the kidney in response to UUO[11, 16, 22, 23]. To confirm the hematopoietic origin of these fibroblasts, we generated chimeric mice that express GFP driven by collagen α1(I) promoter. Two months after bone marrow transplantation, chimeric mice were subjected to UUO. Kidney sections were stained for CD45 or CD11b, and examined with a fluorescence microscope. GFP and CD45 or CD11b dual positive cells were detected abundantly in the obstructed kidneys, but rarely seen in the contralateral kidneys (Figure 1A–B). These data indicate that bone marrow-derived fibroblasts are of hematopoietic origin.

To assess if bone marrow-derived fibroblasts can proliferate in the kidney, kidney section were stained for Ki-67, a marker of proliferating cells, and examined with a fluorescence

microscope. GFP and Ki-67 dual positive cells were detected abundantly in the obstructed kidneys, but not observed in the contralateral kidneys (Figure 1C). These data indicate that bone marrow-derived fibroblasts are capable of proliferating in the kidney after obstructive injury.

To determine if bone marrow-derived fibroblasts can differentiate into myofibroblasts, kidney sections were stained for α-SMA, a marker of myofibroblasts, and examined with a fluorescence microscope. GFP and α-SMA dual positive cells were detected abundantly in the obstructed kidneys, but not observed in the contralateral kidneys (Figure 1D). These data indicate that bone marrow-derived fibroblasts can differentiate into myofibroblasts in the kidney after obstructive injury.

To examine if bone marrow-derived fibroblasts in the kidney express CXCR6, kidney sections were stained for CXCR6 and examined with a fluorescence microscope. GFP and CXCR6 dual positive cells are detected abundantly in the obstructed kidneys, but rarely seen in the contralateral kidneys (Figure 1E). These results indicate that bone marrow-derived fibroblasts recruited into the kidney express CXCR6.

CXCR6 Deficiency Impairs Myeloid Fibroblasts Accumulation

To examine if CXCR6 plays a role in recruiting bone marrow-derived fibroblasts into the kidney, WT and CXCR6 KO mice were subjected to obstructive injury for 7 days. Kidney sections were stained for CD45 and procollagen I or CD45 and PDGFR-β and examined with a fluorescent microscope. The results showed that the number of $CD45^+$ and procollagen I^+ cells or $CD45^+$ and PDGFR-β^+ cells was significantly reduced in the obstructed kidneys of CXCR6 KO mice compared with WT mice (Figure 2A–D). To further quantify the number of myeloid fibroblasts in the kidney, freshly dispersed kidney cells were stained for CD45 and collagen I, and examined by flow cytometry. $CD45^+$ and collagen I^+ cells constituted 45% of total collagen I^+ cells in obstructed kidneys of WT mice. CXCR6 deficiency significantly suppressed $CD45^+$ and collagen I^+ cell accumulation in obstructed kidneys (Figure 2E–F). These data indicate that CXCR6 plays an important role in recruiting bone marrow-derived fibroblasts into the kidney after obstructive injury.

CXCR6 Deficiency Reduces Profibrotic Chemokine and Cytokine Expression

We have recently demonstrated that the presence and development of bone marrow-derived fibroblasts from a $CD45^+$ mononuclear cell population is driven by the induction of the chemokines - CXCL16 and MCP-1[11, 24]. We therefore examined if CXCR6 deficiency affected CXCL16 and MCP-1 gene expression. CXCR6 deficiency inhibited CXCL16 and MCP-1 mRNA expression in the kidney in response to obstructive injury (Figure 3A–B). These data indicate that there is an interaction between CXCL16/CXCR6 and MCP-1/CCR2.

Besides directly produces extracellular matrix, bone marrow-derived fibroblasts have been reported to promote fibrosis indirectly through production of profibrotic cytokines[25–27]. We then examined if CXCR6 deficiency influenced the expression of TNF-α and TGF-β, two major profibrotic cytokines. CXCR6 deficiency suppressed TNF-α and TGF-β mRNA expression in obstructed kidneys (Figure 3C–D).

CXCR6 Deficiency Reduces Myofibroblast Formation

To determine if CXCR6 deficiency affects myofibroblast formation in the kidney, kidney sections were stained for α-SMA, a marker of myofibroblasts, and examined with a fluorescent microscope. CXCR6 deficiency resulted in a significant reduction in the number of myofibroblasts in the obstructed kidneys compared with WT mice (Figure 4AB). Consistent with these findings, Western blot analysis showed that CXCR6 deficiency significantly reduced the protein expression levels of α-SMA in the obstructed kidneys compared with WT mice (Figure 4 C–D). These results indicate that CXCR6 deficiency reduces myofibroblast population in the kidney in response to obstructive injury.

CXCR6 Deficiency Suppresses Renal Fibrosis

Since CXCR6 regulates the accumulation of bone marrow-derived fibroblasts in the kidney in response to obstructive injury, we then examined the effect of CXCR6 deficiency on the development of renal interstitial fibrosis. WT and CXCR6 KO mice were subjected to UUO for 14 days. WT mice developed significant collagen deposition in the obstructed kidneys as demonstrated by positive Sirius red staining, whereas this fibrotic response was significantly attenuated in the obstructed kidneys of CXCR6 KO mice (Figure 5). These data indicate that CXCR6 plays a critical role in the pathogenesis of renal fibrosis.

We next investigated the effect of CXCR6 deficiency on the expression and accumulation of collagen I and fibronectin, two major components of extracellular matrix. There was a marked increase in the protein expression levels of collagen I and fibronectin in the obstructed kidneys of WT mice. In contrast, CXCR6 deficiency significantly suppressed the protein expression levels of these extracellular matrix proteins in the obstructed kidneys (Figure 6). These data indicate that CXCR6 deficiency attenuates renal fibrosis by inhibiting production and deposition of extracellular matrix proteins.

CXCR6 Deficiency in Bone Marrow-derived Fibroblasts Inhibits Renal Fibrosis

To dissect the role of CXCR6 in bone marrow-derived cells in the development of renal fibrosis, we performed bone marrow transplant of WT or KO mice with $CXCR6^{+/+}$ or $CXCR6^{-/-}$ bone marrow cells. Eight weeks after bone marrow transplantation, chimeric mice were subjected to UUO. The genotype of bone marrow-derived cells from the chimeric mice was confirmed by PCR of DNA extracted from peripheral blood cells (Figure S1). Compared with WT mice transplanted with $CXCR6^{+/+}$ bone marrow cells, WT mice transplanted with $CXCR6^{-/-}$ bone marrow cells accumulated fewer bone marrow-derived fibroblasts and displayed a lesser degree of interstitial fibrosis (Figure 7). In contrast, transplant of $CXCR6^{+/+}$ bone marrow into $CXCR6^{-/-}$ recipients restored recruitment of myeloid fibroblasts and susceptibility to fibrosis (Figure 7). These data indicate that CXCR6 signaling in bone marrow-derived cells is important for recruitment of myeloid fibroblasts and development of renal interstitial fibrosis.

CXCR6 Deficiency Inhibits Myeloid Fibroblast Accumulation and Renal Fibrosis after Ischemia-Reperfusion Injury

We have demonstrated that CXCR6 signaling recruits myeloid fibroblasts into the kidney and the development of renal interstitial fibrosis induced by obstructive injury, we next

examined whether CXCR6 signaling regulates myeloid fibroblast infiltration and fibrosis development in a different fibrosis model. We performed ischemia-reperfusion injury (IRI) using a 45-minute warm ischemia time to induce fibrosis. CXCL16 was induced in the kidney following IRI (Figure 8A). CXCR6 KO mice displayed significantly fewer $CD45^+$ myeloid fibroblasts in the kidneys with IRI compared with WT mice at day 7 after IRI (Figure 8B–C). Consistent with these findings, WT mice exhibited prominent interstitial collagen deposition at day14 after IRI. In contrast, CXCR6 KO mice showed much less degree of interstitial collagen deposition following IRI (Figure 8D–E).

DISCUSSION

Tubulointerstitial fibrosis is a hallmark of progressive kidney disease and is central to the loss of renal function after kidney injury. However, the origin of the fibroblasts that are responsible for the excessive production and deposition of extracellular matrix remains a subject of intense debate. Recent studies provide strong evidence that bone marrow-derived fibroblasts are recruited into the kidney and contribute significantly to the pathogenesis of renal interstitial fibrosis[7, 10, 11, 23, 28, 29]. However, not all studies support the bone marrow origin of fibroblasts in renal fibrosis. It has been reported that bone marrow-derived cells do not contribute significantly to collagen synthesis[29]. This may be due to the use of different tracing strategy. In the present study, our results show that bone marrow-derived fibroblasts are of hematopoietic origin. These cells can proliferate and transform into myofibroblasts in the kidney following obstructive injury. Flow cytometric analysis reveals that $CD45^+$ and collagen I^+ cells constitute 45% of the total collagen$^+$ fibroblast population.

Bone marrow-derived fibroblast precursors are derived from a subpopulation of circulating mononuclear cells[13, 30, 31]. We and others have shown that these cells migrate into the kidney in response to obstructive injury and contribute significantly to the development of renal fibrosis[8, 11, 12, 14, 16, 32]. However, the signaling mechanisms underlying the recruitment of these myeloid fibroblast precursors into the kidney are incompletely understood. Bone marrow-derived fibroblasts express certain chemokine receptors such as CCR2, CCR5, CCR7, CXCR6, and CXCR4 in different organs and conditions[11, 18, 19, 33]. In the present study, we show that bone marrow-derived fibroblasts in the kidney express CXCR6. We demonstrate that CXCR6 signaling is pathologically important because genetic deletion of CXCR6 inhibits bone marrow-derived fibroblast and myofibroblast accumulation in the kidney. It is noted that targeted disruption of CXCR6 does not completely prevent $CD45^+$ myeloid fibroblast infiltration into the kidney. This can be explained by the observation that bone marrow-derived fibroblast precursors express chemokine receptors other than CXCR6[19]. Indeed, CCR2 and CCR7 have been reported to regulate myeloid fibroblast recruitment in response to obstructive injury[8, 12, 23].

We have recently shown that CXCL16 is induced in tubular epithelial cells in response to obstructive injury and disruption of CXCL16 inhibits bone marrow-derived fibroblast recruitment into the kidney and renal fibrosis development[11]. We and others have also shown that MCP-1/CCR2 axis plays an important role in recruitment of bone marrow-derived fibroblasts into the kidney and development of renal fibrosis[12, 23]. These studies indicate that these chemokines and their receptors are interactive. In the present study, we

have shown that CXCR6 deficiency reduces CXCL16 and MCP-1 gene expression in the kidney. This can be explained by the observation that CXCR6 deficiency inhibits TNF-α expression in the kidney. Bone marrow-derived fibroblasts express TNF-α[25] and TNF-α can stimulate CXCL16 and MCP-1 gene expression in tubular epithelial cells[23]. Furthermore, our results have shown that CXCR6 deficiency suppresses TGF-β1 expression in the kidney and TGF-β1 can promote myeloid fibroblast differentiation[19]. These data indicate that CXCR6 signaling not only plays an important role in recruiting myeloid fibroblast precursors into the kidney, but also regulates activation of myeloid fibroblast precursors and resident fibroblasts via profibrotic cytokine expression.

A key pathological feature of renal interstitial fibrosis is the prominent increase and deposition of extracellular matrix proteins including collagens and fibronectin. Morphometric analysis of Sirius red staining of kidney sections at day 14 after obstructive injury demonstrates significant presence of interstitial collagen deposition in obstructed kidneys of WT mice. This collagen deposition is significantly attenuated in obstructed kidneys of CXCR6 KO mice. Consistent with these findings, we further demonstrate that the expression of two major ECM proteins, fibronectin and collagen I, are markedly increased in obstructed kidneys of WT mice; these fibrotic responses are significantly attenuated in obstructed kidneys of CXCR6 KO mice.

The magnitude of the fibrotic response correlates with the absolute number of $CD45^+$ myeloid fibroblasts that are recruited into the interstitial space in response to obstructive injury. WT mice accumulate a large number of $CD45^+$ myeloid fibroblasts and develop severe fibrosis after obstructive injury. In contrast, CXCR6 KO mice accumulate significantly fewer $CD45^+$ myeloid fibroblasts into the kidney and develop much less degree of renal interstitial fibrosis. Furthermore, compared with WT mice transplanted with $CXCR6^{+/+}$ bone marrow cells, WT mice transplanted with $CXCR6^{-/-}$ bone marrow cells accumulate fewer $CD45^+$ myeloid fibroblasts and develop a lesser amount of renal interstitial fibrosis. CXCR6 KO mice transplanted with $CXCR6^{+/+}$ bone marrow cells restores both $CD45^+$ myeloid fibroblast recruitment and fibrotic susceptibility. These data provide compelling evidence for an important role of bone marrow-derived, CXCR6-expressing fibroblasts in the development of fibrotic responses after obstructive injury. CXCR6 deficiency does not completely abolish the fibrotic response, which are consistent with other chemokines and their receptors, such as MCP-1/CCR2 contribute to development of renal fibrosis[12, 23]. Besides regulating the recruitment of myeloid fibroblasts into the kidney, CXCR6 signaling may affect cell death, inflammation, or fibroblast activation, which requires further investigation.

Renal ischemia-reperfusion injury is a major cause of acute kidney injury (AKI) and an important determinant of long term kidney dysfunction. As many as 50% patients with severe AKI ultimately develop prominent structural alterations including renal interstitial fibrosis. A recent study has shown that post-ischemic kidney environment is profibrotic and more than 30% of interstitial α-SMA positive myofibroblasts are derived from the bone marrow[10]. However, the mechanisms underlying the recruitment of the bone marrow-derived fibroblasts are incompletely understood. In the present study, we have demonstrated that CXCL16 is induced in response to ischemia-reperfusion injury and CXCR6 deficiency

inhibits $CD45^+$ myeloid fibroblast accumulation and attenuates renal fibrosis development, suggesting that CXCR6 signaling plays an important role in recruiting bone marrow-derived fibroblast precursors into the kidney and the pathogenesis of renal fibrosis after ischemia-reperfusion injury and is a potential therapeutic target for the treatment of post-ischemic fibrotic kidney disease.

In conclusion, our study defines a novel mechanism by which CXCR6 regulates the pathogenesis of renal fibrosis. In response to injury, CXCR6 recruits $CD45^+$ myeloid fibroblasts into the kidney, which contribute significantly to the development of renal interstitial fibrosis. These data suggest that inhibition of CXCR6 signaling represents a novel therapeutic strategy for the treatment of fibrotic kidney disease.

METHODS

Animals

Animal experiments were approved by the Institutional Animal Care and Use Committee of Baylor College of Medicine. The investigation conforms with the Guide for the Care and Use of Laboratory Animals published by the US National Institutes of Health (NIH Publication No. 85-23, revised 1996). The CXCR6 KO mice on a background of C57BL/6J were purchased from the Jackson Laboratory. Transgenic mice, expressing GFP driven by collagen α1(I) promoter (Col), were a generous gift from Dr. DA Brenner[34]. Male WT or CXCR6 KO mice at 8–12 weeks old, weighing 20–30 g were used for the study. The UUO procedure was performed as described[11, 16, 22, 23]. To induce unilateral ischemia-reperfusion injury, left kidneys were exposed through flank incision and were subjected to ischemia by clamping renal pedicles with non-traumatic micro aneurysm clamps as described[16]. Mice were allowed to recover from anesthesia and were housed in standard rodent cages with *ad libitum* access to water and food until sacrificed.

Bone Marrow Transplantation

Bone marrow transplantation was performed as described previously[11, 23, 35]. Briefly, bone marrow cells (5×10^6) from CoI1A1-GFP mice were transferred to lethally irradiated C57BL/6 mice. Chimeric mice were allowed to recuperate for 2 months prior to induction of kidney injury by UUO.

Renal Morphology

Mice were euthanized and perfused with PBS to remove blood. One portion of the kidney tissue was fixed in 10% buffered formalin and embedded in paraffin, cut at 4 Lm thickness, and stained with Sirius red to identify collagen fibers. The Sirius red-stained sections were scanned using a microscope equipped with a digital camera (Nikon Instruments Inc., Melville, NY), and quantitative evaluation was performed using NIS-Elements Br 3.0 software. The Sirius red-stained area was calculated as a percentage of the total area.

Immunofluorescence

Immunofluorescence staining was performed as described[11]. Briefly, frozen kidney sections were fixed and nonspecific binding was blocked with protein block (Dako, Carpinteria, CA).

Slides were then incubated with rat anti-CD45 antibody, rat anti-CD11b antibody (BD Biosciences, San Jose, CA), rabbit anti-Ki-67 antibody (Cell Signaling, Danvers, MA), rat anti-CXCR6 antibody (R&D Systems, Minneapolis, MN), rabbit anti-collagen I antibody (Rockland Immunochemicals, Gilbertsville, PA), rabbit anti-fibronectin antibody (Sigma-Aldrich, St. Louis, MO) or rabbit anti-α-SMA antibody (Abcam, Cambridge, MA) followed by appropriate fluorescence-conjugated secondary antibodies (Invitrogen, Carlsbad, CA). For double immunofluorescence, kidney sections were fixed and stained with primary antibodies followed by appropriate secondary antibodies sequentially. Slides were mounted with mounting medium containing DAPI. Fluorescence intensity was visualized using a microscope equipped with a digital camera (Nikon Instruments Inc., Melville, NY). Quantitative evaluation of sections stained with antibodies to α-SMA, collagen I and fibronectin was performed using NIS-Elements Br 3.0 software. The fluorescence positive area was calculated as a percentage of the total area.

Renal Cell Isolation and Flow Cytometry

Renal cell isolation and flow cytometry were performed as described[11]. Briefly, kidney was minced and incubated at 37°C for 30 minutes in PBS containing Liberase TM (Roche) and DNase (Roche). Cells were filtered through a 40Lm strainer, washed, centrifuged and resuspended in FACS buffer. Cells (5×10^5) were fixed and permeabilized using the Cytofix/Cytoperm kit (BD Biosciences, San Jose, CA) in accordance with the manufacturer's protocol, then incubated with PE-anti-CD45 (BD Biosciences, San Jose, CA) and biotin-anti-collagen I (Rockland, Gilbertsville, PA)/streptavidin-APC (BD Biosciences, San Jose, CA). Cells incubated with irrelevant isotype-matched antibodies (BD Biosciences, San Jose, CA) and unstained cells were used as controls. The cutoffs were set according to results of controls. The fluorescence intensities were measured using a BD LSR II flow cytometer (BD Biosciences, San Jose, CA). Data were analyzed using BD FACSDiva software.

Real-time RT-PCR

Quantitative analysis of the target mRNA expression was performed with real-time reverse transcription – polymerase chain reaction (RT-PCR) by the relative standard curve method[11]. Total RNA was extracted from snap-frozen kidney tissues with TRIzol Reagent (Invitrogen). Total RNA was reverse-transcribed and amplified in triplicate using IQ SYBR green supermix reagent (Bio-Rad, Herculus, CA) with a real-time PCR machine (Bio-Rad, Herculus, CA), according to the manufacturer's instructions. The specificity of real-time PCR was confirmed by melting-curve analysis. The expression levels of the target genes were normalized to the GAPDH level in each sample. The following are the primer sequences: MCP-1: Forward 5′-TCACCTGCTGCTACTCATTCACCA-3′ and reverse 5′-TACAGCTTCTTTGGGACACCTGCT-3′; CXCL16: Forward 5′-ACCCTTGTCTCTTGCGTTCTTCCT-3′ and reverse 5′-ATGTGATCCAAAGTACCCTGCGGT-3′; TNF-α: Forward 5′-CATGAGCACAGAAAGCATGATCCG-3′ and reverse 5′-AAGCAGGAATGAGAAGAGGCTGAG-3′; TGF-β1: Forward 5′-CAACAATTCCTGGCGTTACCTTGG-3′ and reverse 5′-GAAAGCCCTGTATTCCGTCTCCTT-3′; GAPDH: Forward 5′-

TGCTGAGTATGTCGTGGAGTCTA-3′ and reverse 5′-AGTGGGAGTTGCTGTTGAAATC-3′.

Western Blot Analysis

Protein was extracted using the RIPA buffer containing cocktail proteinase inhibitors (Thermo Fisher Scientific Inc., Rockford, IL) and quantified with Bio-Rad protein assay. Equal amounts of protein were separated on SDS–polyacrylamide gels in a Tris/glycine buffer system, transferred onto nitrocellulose membranes, and blotted according to standard procedures with primary antibodies (collagen I, fibronectin, and α-SMA) followed by appropriate secondary antibodies. Membranes were reblotted with anti-GAPDH antibody (Millipore, Billerica, CA). The specific bands of target proteins were analyzed using an Odyssey IR scanner (LI-COR Bioscience, Lincoln, NE) and band intensities were quantified using NIH Image/J.

Statistical Analysis

All data were expressed as mean ± SEM. Multiple group comparisons were performed by one-way ANOVA followed by the Bonferroni procedure for comparison of means. $P < 0.05$ was considered statistically significant.

Supplementary Material

Refer to Web version on PubMed Central for supplementary material.

ACKNOWLEDGMENTS

We thank Dr. William E. Mitch for critical reading of the manuscript and Joel M. Sederstrom for expert assistance with flow cytometry. We also thank Drs. David A. Brenner and Tatiana Kisseleva at University of California - San Diego for providing collagen I-GFP mice. This work was supported in part by the NIH grants – K08HL092958 and R01DK095835 and an AHA grant - 11BGIA7840054 to YW. J Yan was supported by a NIH training grant T32DK062706. ML Entman was supported by a NIH grant R01HL089792. The Cytometry and Cell Sorting Core at Baylor College of Medicine was supported by the NIH grant - AI036211, CA125123, and RR024574.

References

1. Levey AS, Atkins R, Coresh J, et al. Chronic kidney disease as a global public health problem: approaches and initiatives - a position statement from Kidney Disease Improving Global Outcomes. Kidney Int. 2007; 72:247–259. [PubMed: 17568785]
2. Schainuck LI, Striker GE, Cutler RE, et al. Structural-functional correlations in renal disease. II. The correlations. Hum Pathol. 1970; 1:631–641. [PubMed: 5521736]
3. Nath KA. The tubulointerstitium in progressive renal disease. Kidney Int. 1998; 54:992–994. [PubMed: 9734628]
4. Neilson EG. Mechanisms of disease: Fibroblasts--a new look at an old problem. Nat Clin Pract Nephrol. 2006; 2:101–108. [PubMed: 16932401]
5. Strutz F, Muller GA. Renal fibrosis and the origin of the renal fibroblast. Nephrol Dial Transplant. 2006; 21:3368–3370. [PubMed: 16887850]
6. Liu Y. Renal fibrosis: new insights into the pathogenesis and therapeutics. Kidney Int. 2006; 69:213–217. [PubMed: 16408108]
7. Li J, Deane JA, Campanale NV, et al. The contribution of bone marrow-derived cells to the development of renal interstitial fibrosis. Stem Cells. 2007; 25:697–706. [PubMed: 17170067]

8. Sakai N, Wada T, Yokoyama H, et al. Secondary lymphoid tissue chemokine (SLC/CCL21)/CCR7 signaling regulates fibrocytes in renal fibrosis. Proc Natl Acad Sci U S A. 2006; 103:14098–14103. [PubMed: 16966615]
9. Grimm PC, Nickerson P, Jeffery J, et al. Neointimal and tubulointerstitial infiltration by recipient mesenchymal cells in chronic renal-allograft rejection. N Engl J Med. 2001; 345:93–97. [PubMed: 11450677]
10. Broekema M, Harmsen MC, van Luyn MJ, et al. Bone marrow-derived myofibroblasts contribute to the renal interstitial myofibroblast population and produce procollagen I after ischemia/reperfusion in rats. J Am Soc Nephrol. 2007; 18:165–175. [PubMed: 17135399]
11. Chen G, Lin SC, Chen J, et al. CXCL16 recruits bone marrow-derived fibroblast precursors in renal fibrosis. J Am Soc Nephrol. 2011; 22:1876–1886. [PubMed: 21816936]
12. Reich B, Schmidbauer K, Rodriguez Gomez M, et al. Fibrocytes develop outside the kidney but contribute to renal fibrosis in a mouse model. Kidney Int. 2013; 84:78–89. [PubMed: 23486523]
13. Bucala R, Spiegel LA, Chesney J, et al. Circulating fibrocytes define a new leukocyte subpopulation that mediates tissue repair. Mol Med. 1994; 1:71–81. [PubMed: 8790603]
14. Niedermeier M, Reich B, Rodriguez Gomez M, et al. CD4+ T cells control the differentiation of Gr1+ monocytes into fibrocytes. Proc Natl Acad Sci U S A. 2009; 106:17892–17897. [PubMed: 19815530]
15. Shao DD, Suresh R, Vakil V, et al. Pivotal Advance: Th-1 cytokines inhibit, and Th-2 cytokines promote fibrocyte differentiation. Journal of leukocyte biology. 2008; 83:1323–1333. [PubMed: 18332234]
16. Yang J, Lin SC, Chen G, et al. Adiponectin Promotes Monocyte-to-Fibroblast Transition in Renal Fibrosis. J Am Soc Nephrol. 2013 In Press.
17. Metz CN. Fibrocytes: a unique cell population implicated in wound healing. Cell Mol Life Sci. 2003; 60:1342–1350. [PubMed: 12943223]
18. Quan TE, Cowper S, Wu SP, et al. Circulating fibrocytes: collagen-secreting cells of the peripheral blood. Int J Biochem Cell Biol. 2004; 36:598–606. [PubMed: 15010326]
19. Abe R, Donnelly SC, Peng T, et al. Peripheral blood fibrocytes: differentiation pathway and migration to wound sites. J Immunol. 2001; 166:7556–7562. [PubMed: 11390511]
20. Cieslik KA, Taffet GE, Carlson S, et al. Immune-inflammatory dysregulation modulates the incidence of progressive fibrosis and diastolic stiffness in the aging heart. Journal of molecular and cellular cardiology. 2011; 50:248–256. [PubMed: 20974150]
21. Murphy PM. The molecular biology of leukocyte chemoattractant receptors. Annu Rev Immunol. 1994; 12:593–633. [PubMed: 8011292]
22. Yang J, Chen J, Yan J, et al. Effect of interleukin 6 deficiency on renal interstitial fibrosis. PLoS One. 2012; 7:e52415. [PubMed: 23272241]
23. Xia Y, Entman ML, Wang Y. CCR2 Regulates the Uptake of Bone Marrow-Derived Fibroblasts in Renal Fibrosis. PLoS One. 2013; 8:e77493. [PubMed: 24130892]
24. Haudek SB, Cheng J, Du J, et al. Monocytic fibroblast precursors mediate fibrosis in angiotensin-II-induced cardiac hypertrophy. J Mol Cell Cardiol. 2010; 49:499–507. [PubMed: 20488188]
25. Chesney J, Metz C, Stavitsky AB, et al. Regulated production of type I collagen and inflammatory cytokines by peripheral blood fibrocytes. J Immunol. 1998; 160:419–425. [PubMed: 9551999]
26. Wang J, Jiao H, Stewart TL, et al. Accelerated wound healing in leukocytespecific, protein 1-deficient mouse is associated with increased infiltration of leukocytes and fibrocytes. J Leukoc Biol. 2007; 82:1554–1563. [PubMed: 18040084]
27. Duerrschmid C, Crawford JR, Reineke E, et al. TNF receptor 1 signaling is critically involved in mediating angiotensin-II-induced cardiac fibrosis. J Mol Cell Cardiol. 2013; 57:59–67. [PubMed: 23337087]
28. Iwano M, Plieth D, Danoff TM, et al. Evidence that fibroblasts derive from epithelium during tissue fibrosis. J Clin Invest. 2002; 110:341–350. [PubMed: 12163453]
29. Roufosse C, Bou-Gharios G, Prodromidi E, et al. Bone marrow-derived cells do not contribute significantly to collagen I synthesis in a murine model of renal fibrosis. J Am Soc Nephrol. 2006; 17:775–782. [PubMed: 16467445]

30. Chesney J, Bacher M, Bender A, et al. The peripheral blood fibrocyte is a potent antigen-presenting cell capable of priming naive T cells in situ. Proc Natl Acad Sci U S A. 1997; 94:6307–6312. [PubMed: 9177213]

31. Chesney J, Bucala R. Peripheral blood fibrocytes: novel fibroblast-like cells that present antigen and mediate tissue repair. Biochem Soc Trans. 1997; 25:520–524. [PubMed: 9191147]

32. Xia Y, Entman ML, Wang Y. Critical Role of CXCL16 in Hypertensive Kidney Injury and Fibrosis. Hypertension. 2013; 62:1129–1137. [PubMed: 24060897]

33. Xu J, Lin SC, Chen J, et al. CCR2 mediates the uptake of bone marrow-derived fibroblast precursors in angiotensin II-induced cardiac fibrosis. American journal of physiology Heart and circulatory physiology. 2011; 301:H538–H547. [PubMed: 21572015]

34. Kisseleva T, Uchinami H, Feirt N, et al. Bone marrow-derived fibrocytes participate in pathogenesis of liver fibrosis. J Hepatol. 2006; 45:429–438. [PubMed: 16846660]

35. Jin X, Chen J, Hu Z, et al. Genetic deficiency of adiponectin protects against acute kidney injury. Kidney Int. 2013; 83:604–614. [PubMed: 23302722]

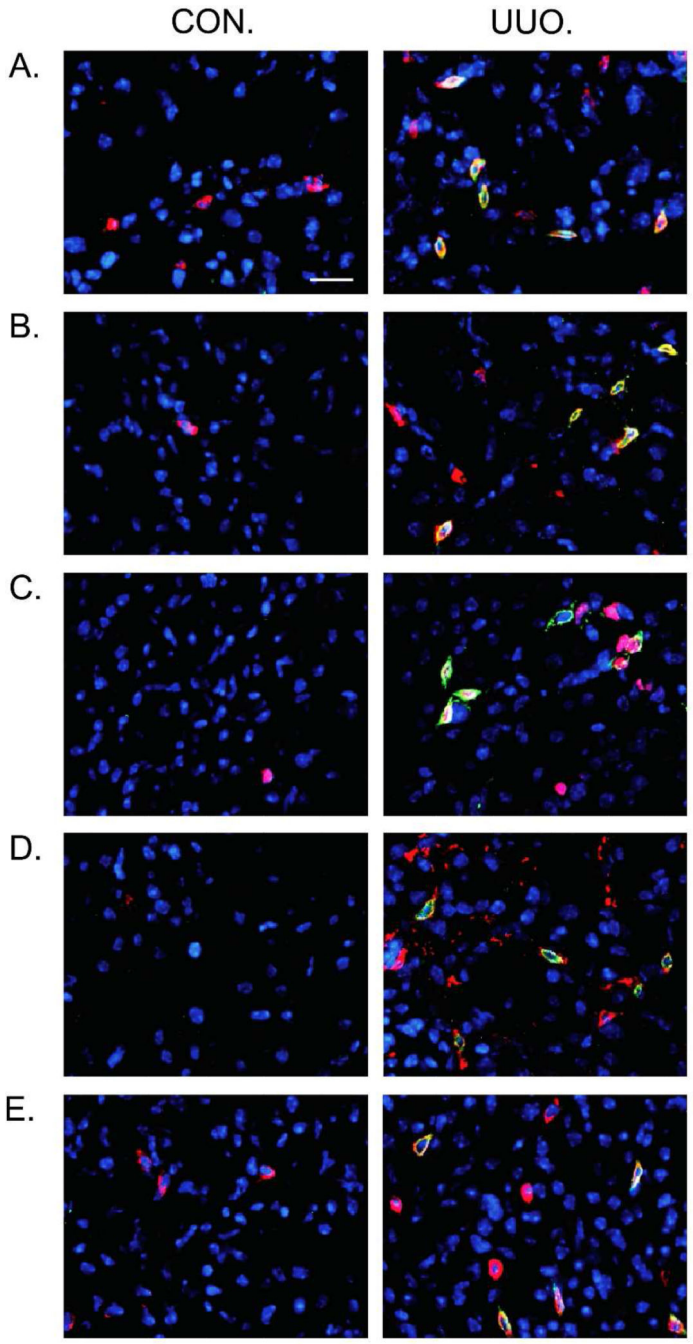

Figure 1. Characterization of bone marrow-derived fibroblasts

A. Representative photomicrographs of kidney sections stained for CD45 (red) and counter stained with DAPI (blue). **B.** Representative photomicrographs of kidney sections stained for CD11b (red) and counter stained with DAPI (blue). **C.** Representative photomicrographs of kidney sections stained for Ki-67 (red) and counter stained with DAPI (blue). **D.** Representative photomicrographs of kidney sections stained for α-SMA (red) and counter stained with DAPI (blue). **E.** Representative photomicrographs of kidney sections stained for CXCR6 (red) and counter stained with DAPI (blue). Scale bar: 25 μm.

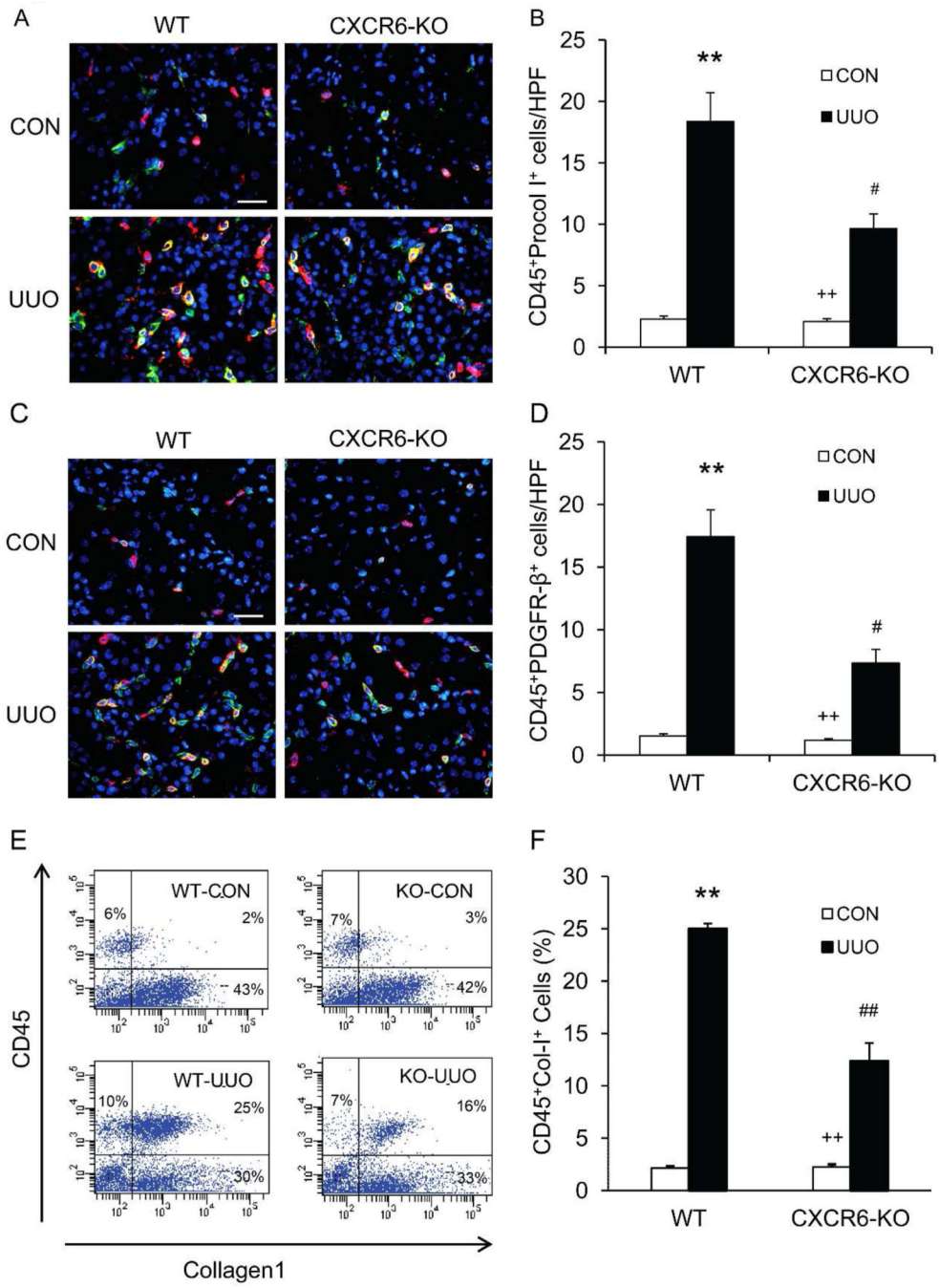

Figure 2. CXCR6 deficiency suppresses the accumulation of bone marrow-derived fibroblasts in the kidney in response to obstructive injury

A. Representative photomicrographs of kidney sections from WT and CXCR6-KO mice 7 days after UUO stained for CD45 (red), procollagen I (green), and DAPI (blue). Scale bar: 25 μm. **B.** Quantitative analysis of $CD45^+$ and procollagen I^+ cells in kidneys of WT and CXCR6-KO mice 7 days after UUO. ** $P < 0.01$ versus WT controls, $^+$ $P < 0.05$ versus KO UUO, and $^\#$ $P < 0.05$ versus WT UUO. n=6 per group. **C.** Representative photomicrographs of kidney sections from WT and CXCR6-KO mice 7 days after UUO stained for CD45

(red), PDGFR-β (green), and DAPI (blue). Scale bar: 25 μm. **D.** Quantitative analysis of $CD45^+$ and PDGFR-β^+ cells in kidneys of WT and CXCR6-KO mice 7 days after UUO. ** $P < 0.01$ versus WT controls, $^+$ $P < 0.05$ versus KO UUO, and $^\#$ $P < 0.05$ versus WT UUO. n=6 per group. **E.** Representative cytometric diagrams showing the effect of CXCR6 deficiency on the accumulation of $CD45^+$ and collagen I^+ cells in the kidneys. **F.** Quantitative analysis of $CD45^+$ and collagen I^+ cells in the kidneys. ** $P < 0.01$ versus WT controls, $^{++}$ $P < 0.01$ versus KO UUO, and $^{\#\#}$ $P < 0.01$ versus WT UUO. n=3 per group.

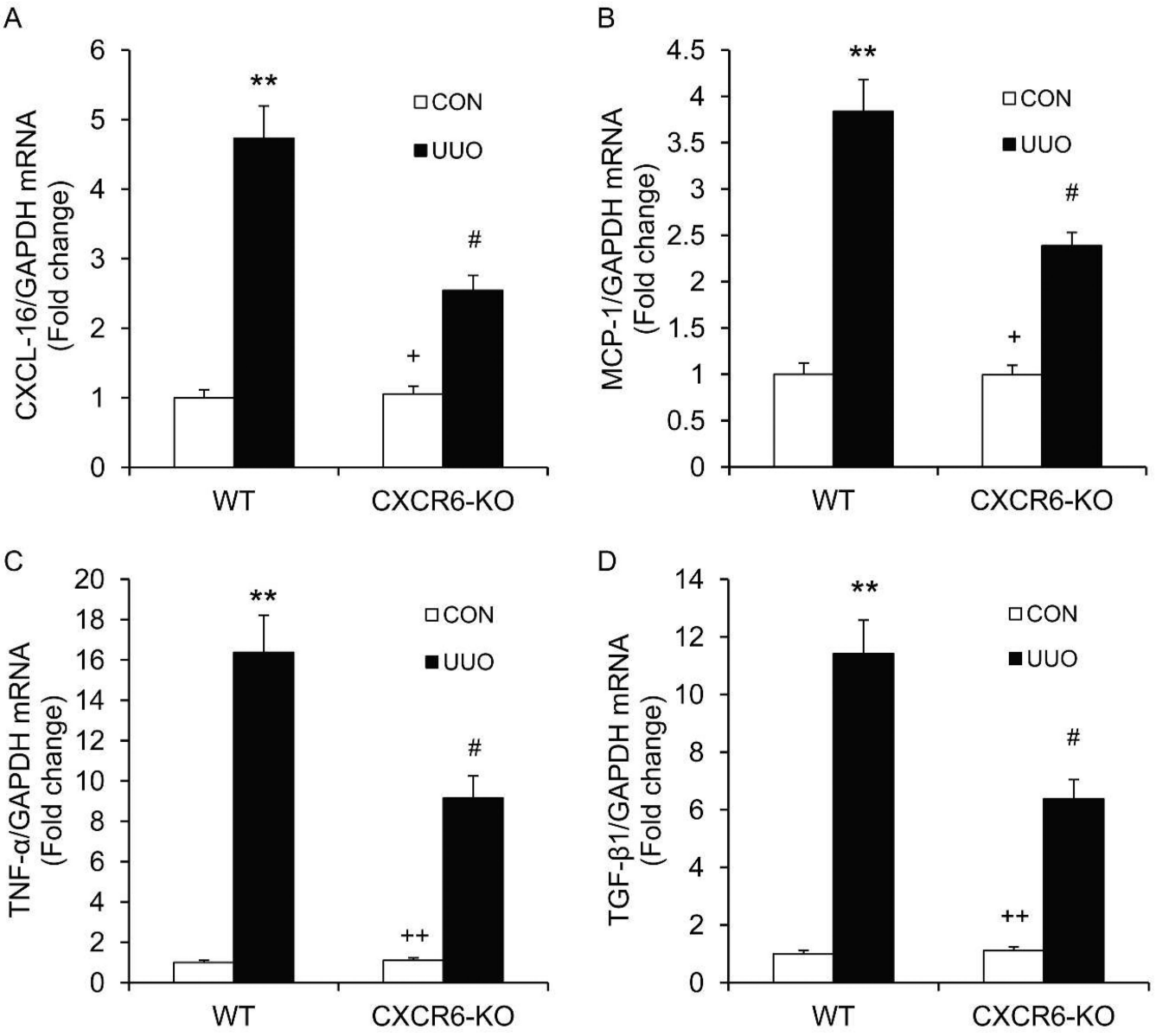

Figure 3. CXCR6 deficiency attenuates profibrotic chemokine and cytokine expression

A. Quantitative analysis of CXCL16 mRNA expression in the kidney. **B.** Quantitative analysis of MCP-1 mRNA expression in the kidney. **C.** Quantitative analysis of TNF-α mRNA expression in the kidney. **D.** Quantitative analysis of TGF-β1 mRNA expression in the kidney. ** P <0.01 versus WT controls, $^{+}$ P <0.05 versus KO UUO, $^{++}$ P <0.01 versus KO UUO, and $^{\#}$ P <0.05 versus WT UUO. n=6 per group.

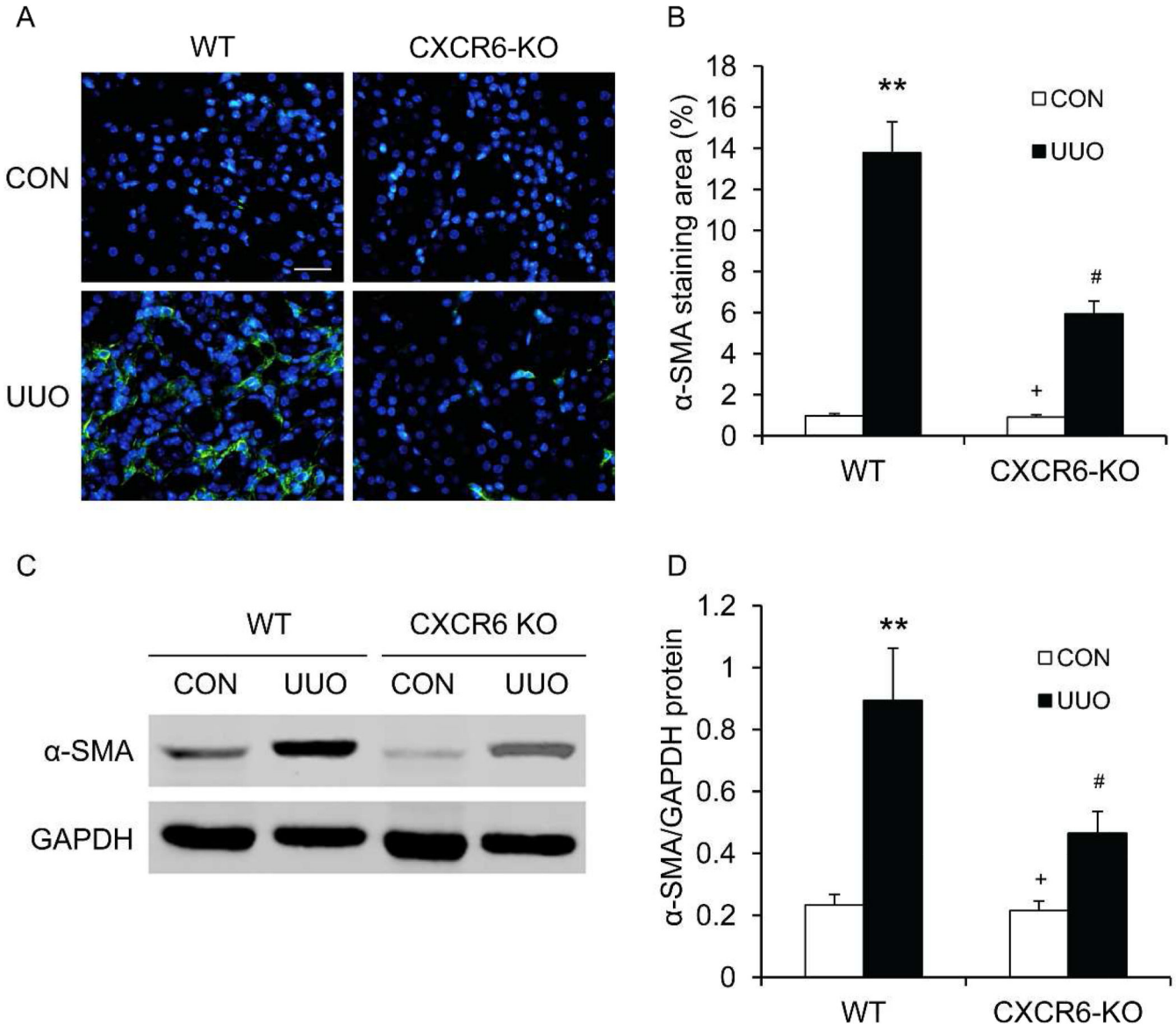

Figure 4. CXCR6 deficiency inhibits myofibroblast activation and α-SMA expression in obstructive nephropathy

A. Representative photomicrographs of α-SMA immunofluorescent staining in kidneys of WT and CXCR6-KO mice 2 weeks after UUO. Scale bar: 25 μm. **B.** Quantitative analysis of α-SMA protein expression in kidneys of WT and CXCR6-KO mice 2 weeks after UUO. ** P <0.01 versus WT controls, $^{+}$ P <0.05 versus KO UUO, and $^{\#}$ P <0.05 versus WT UUO. n=6 per group. **C.** Representative Western blots show the levels of α-SMA protein expression in kidneys of WT and CXCR6-KO mice. **D.** Quantitative analysis of α-SMA protein expression in kidneys of WT and CXCR6-KO mice. ** P <0.01 versus WT controls, $^{+}$ P <0.05 versus KO UUO, and $^{\#}$ P <0.05 versus WT UUO. n=6 per group.

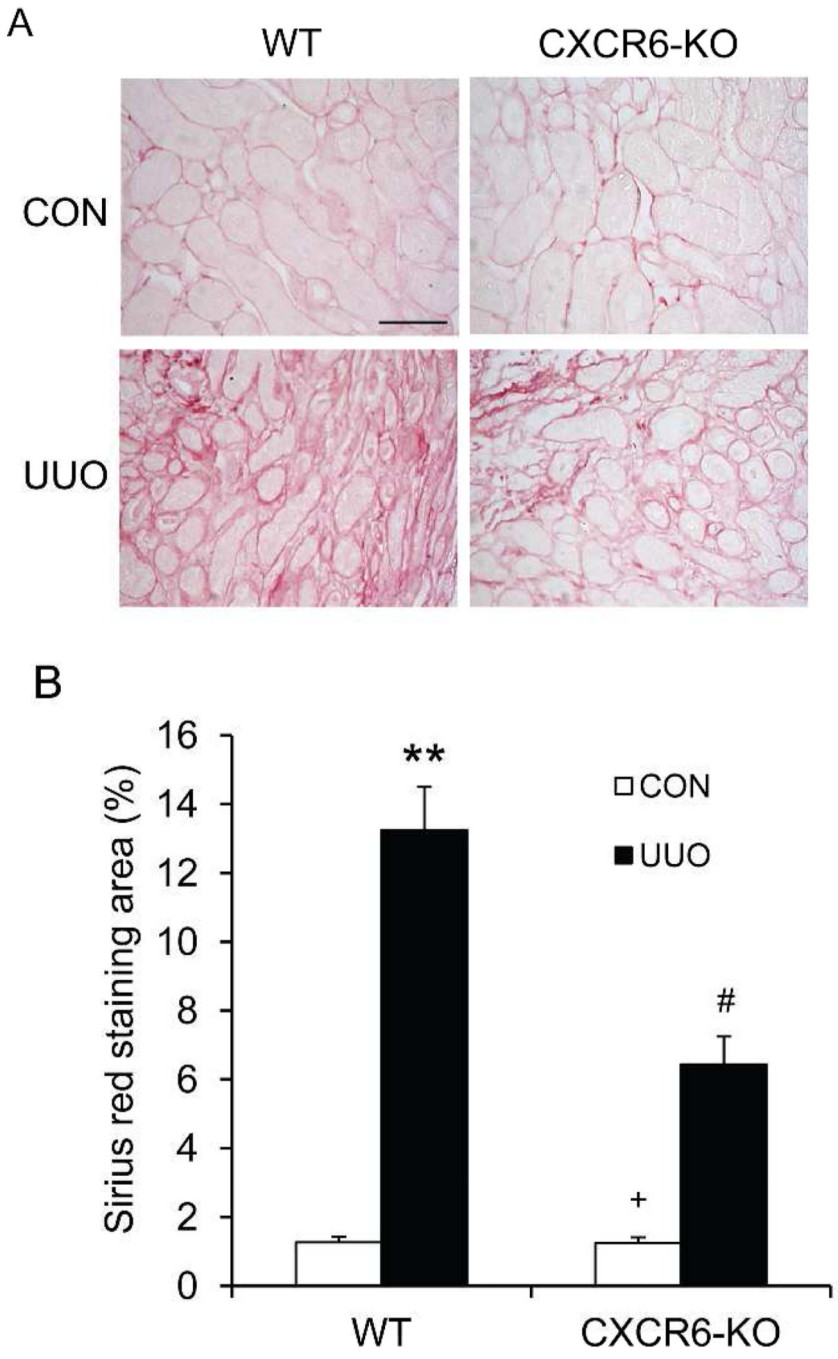

Figure 5. CXCR6 deficiency suppresses renal fibrosis and collagen deposition in the kidney

A. Representative photomicrographs of kidney sections from WT and CXCR6-KO mice 2 weeks after UUO stained with Sirius red. Scale bar: 50 μm. **B.** Quantitative analysis of interstitial collagen content in kidneys. ** $P < 0.01$ versus WT controls, $^{+}$ $P < 0.05$ versus KO UUO, and $^{\#}$ $P < 0.05$ versus WT UUO. n= 6 per group.

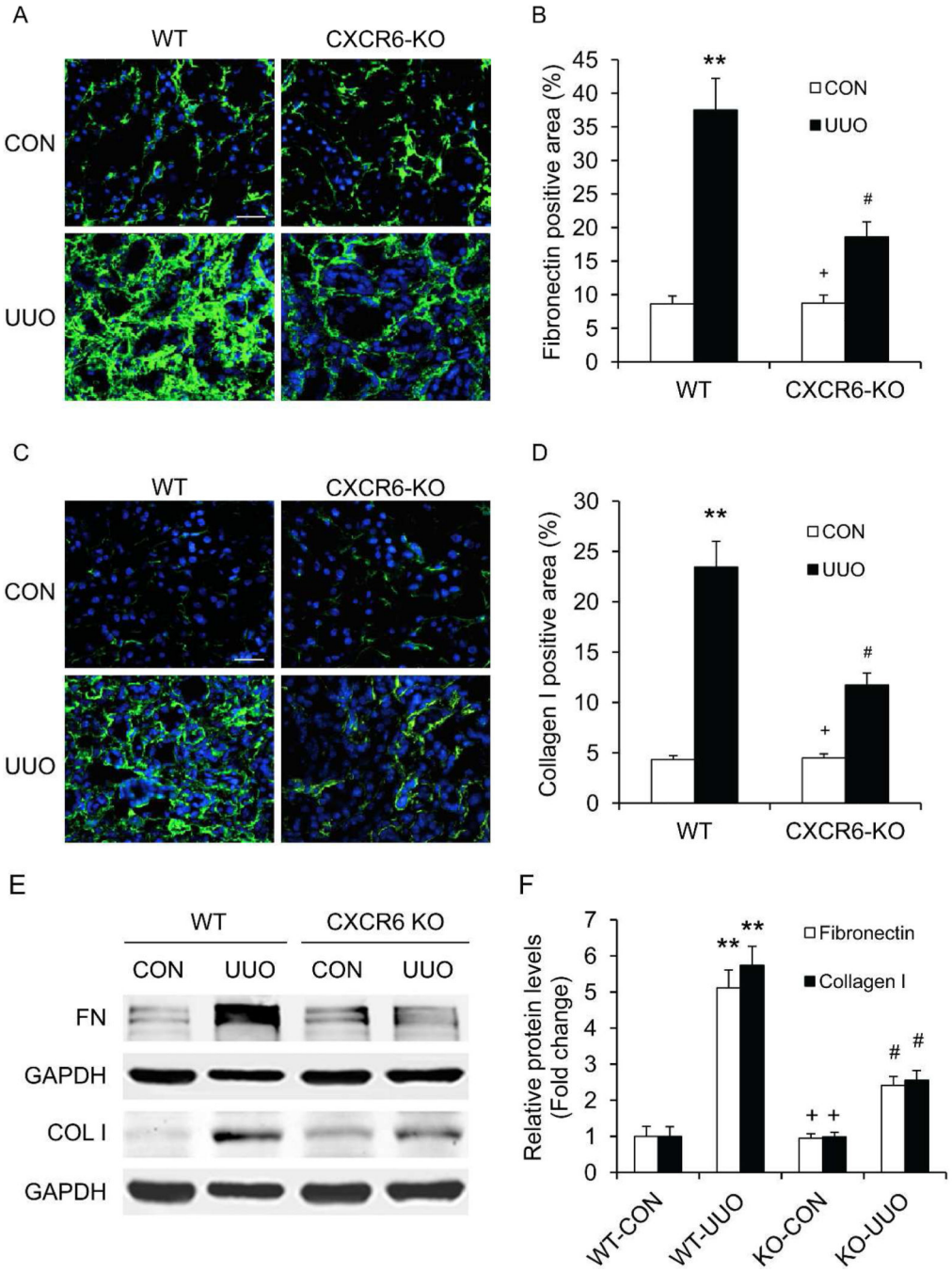

Figure 6. CXCR6 deficiency inhibits fibronectin and collagen I expression in the kidney

A. Representative photomicrographs of fibronectin immunofluorescence staining of kidneys 2 weeks after UUO. Scale bar: 25 μm. **B.** Quantitative analysis of fibronectin positive area of kidneys 2 weeks after UUO. ** P <0.01 versus WT controls, $^{+}$ P <0.05 versus KO UUO, and $^{\#}$ P <0.05 versus WT UUO. n=6 per group. **C.** Representative photomicrographs of collagen I immunofluorescence staining of kidneys 2 weeks after UUO. Scale bar: 25 μm. **D.** Quantitative analysis of collagen I positive area of kidneys 2 weeks after UUO. ** P <0.01 versus WT controls, $^{+}$ P <0.05 versus KO UUO, and $^{\#}$ P <0.05 versus WT UUO. n=6 per

group. **E.** Representative Western blots show the protein levels of fibronectin and collagen I of kidneys 2 weeks after UUO. **F.** Quantitative analysis of fibronectin and collagen I protein expression of kidneys 2 weeks after UUO. * $P < 0.05$ versus WT controls, $^{+}$ $P < 0.05$ versus s KO UUO, and $^{\#}$ $P < 0.05$ versus WT UUO. n=6 per group.

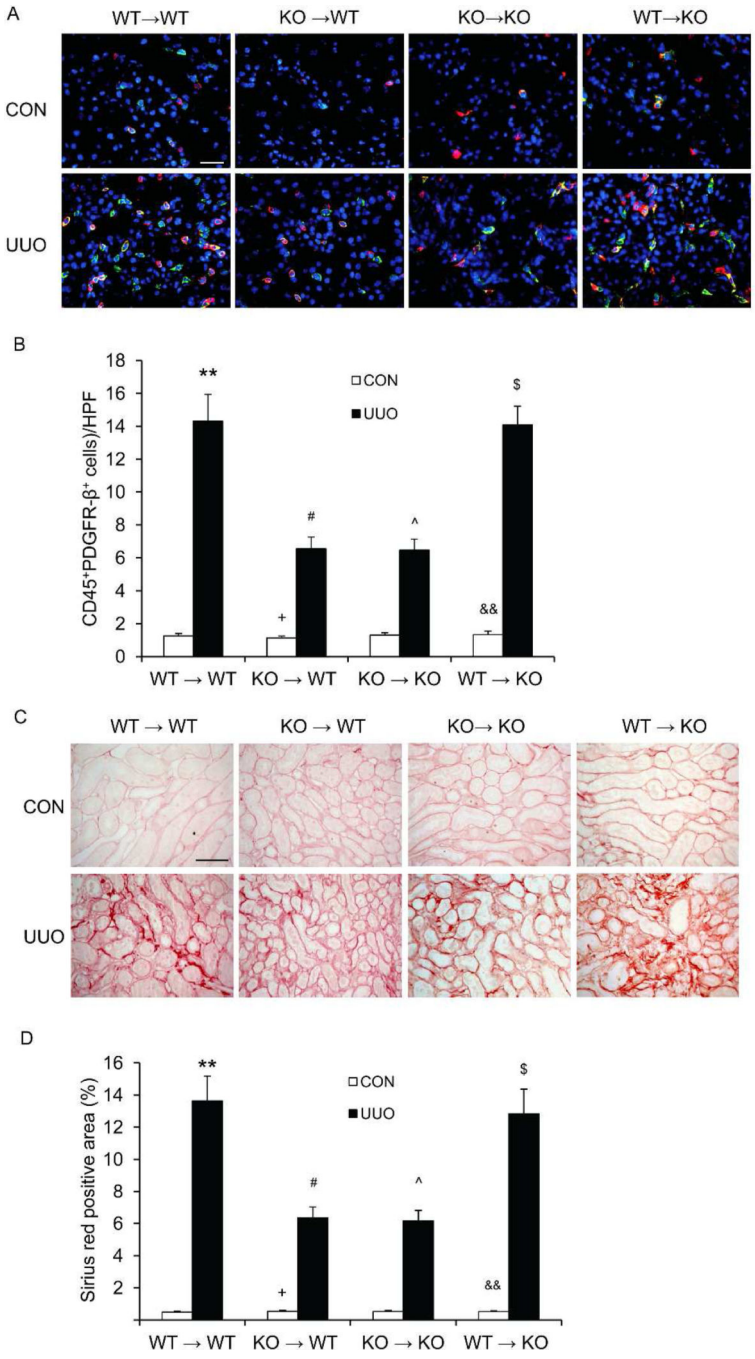

Figure 7. CXCR6 deficiency in bone marrow-derived cells inhibits myeloid fibroblast accumulation and collagen deposition in the kidney

A. Representative photomicrographs of kidney sections from WT or KO mice transplanted with CXCR6$^{+/+}$ or CXCR6$^{-/-}$ bone marrow cells 1 week after UUO stained for CD45 (red), PDGFR-β (green), and DAPI (blue). Scale bar: 25 μm. **B.** Quantitative analysis of CD45^{+} and PDGFR-β^{+} fibroblasts in the kidneys. **p<0.01 versus WT → WT CON; $^{\#}p$<0.05 versus WT → WT UUO; ^{+}p<0.05 versus KO → WT UUO; $^{\wedge}p$<0.05 versus KO→KO CON; $^{\$}$ p<0.05 versus KO→KO UUO; $^{\&\&}$ p<0.01 versus WT→KO UUO. n=5–6 per group.

C. Representative photomicrographs of kidney sections stained with Sirius red. Scale bar: 50 μm. **D.** Quantitative analysis of renal interstitial collagen content in different groups as indicated. $^{**}p<0.01$ versus WT → WT CON; $^{\#}p<0.05$ versus WT → WT UUO; $^{+}p<0.05$ versus KO → WT UUO; $^{\wedge}p<0.05$ versus KO→KO CON; $ $p<0.05$ versus KO→KO UUO; $^{\&\&}$ $p<0.01$ versus WT→KO UUO. n=5–6 per group.

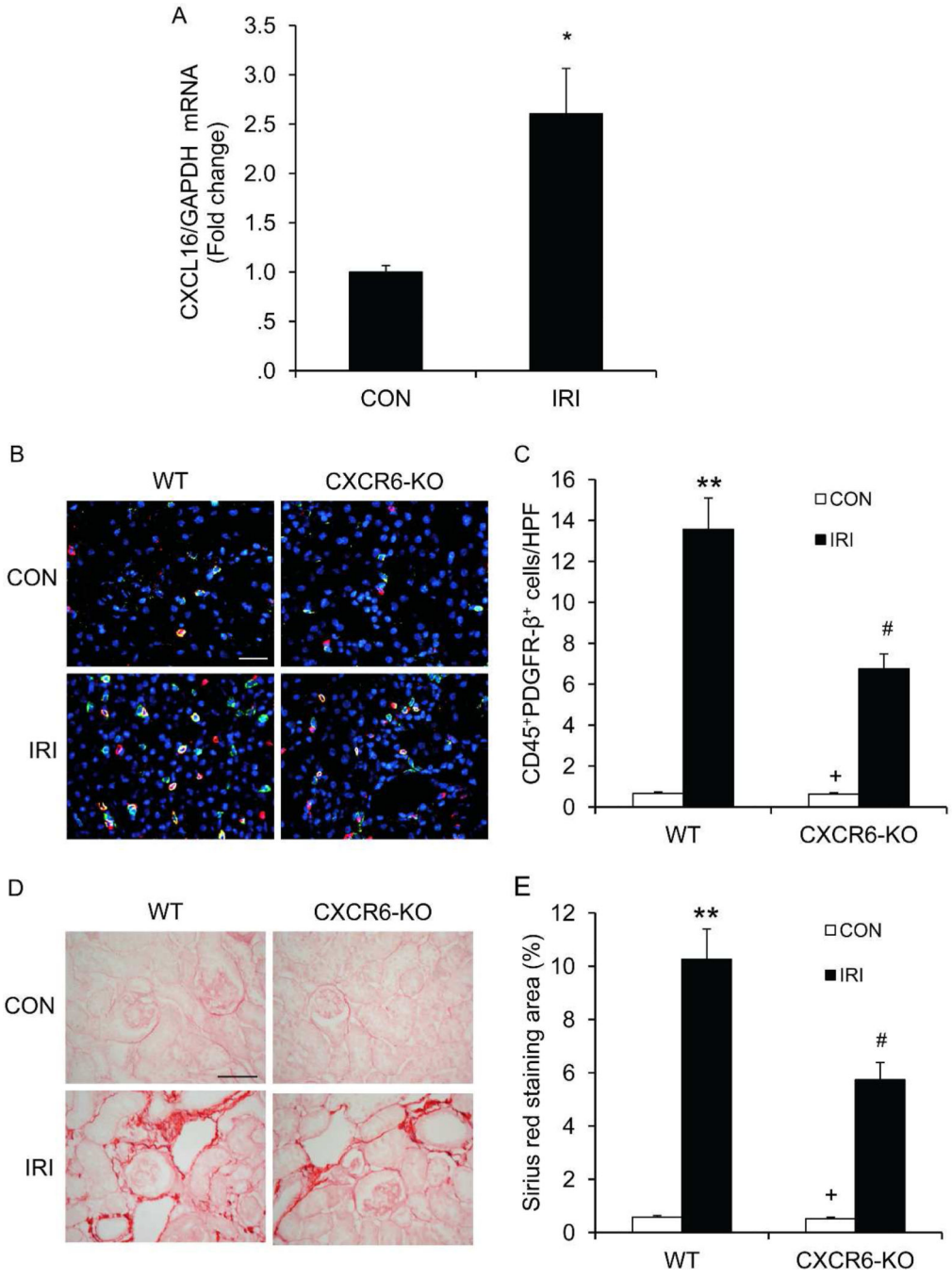

Figure 8. CXCR6 deficiency suppresses bone marrow-derived fibroblast accumulation and collagen deposition in the kidneys in response to IRI

A. CXCL16 is induced in the kidney after IRI. * indicate $p<0.05$ versus sham controls. n=5. **B.** Representative photomicrographs of kidney sections from WT and CXCR6-KO mice 7 days after IRI stained for CD45 (red), PDGFR-β (green), and DAPI (blue). Scale bar: 25 μm. **C.** Quantitative analysis of $CD45^+$ and PDGFR-β^+ cells in the kidneys 7 days after IRI. ** $P < 0.01$ versus WT controls, $^+$ $P < 0.05$ versus KO IRI, and $^\#$ $P < 0.05$ versus WT IRI. n=6 per group. **D.** Representative photomicrographs of kidney sections from WT and CXCR6-

KO mice 2 weeks after IRI stained with Sirius red. Scale bar: 50 μm. **E.** Quantitative analysis of interstitial collagen content in the kidneys. ** $P < 0.01$ versus WT controls, $^{+}$ $P < 0.05$ versus KO IRI, and $^{\#}$ $P < 0.05$ versus WT IRI. n= 6 per group.